International Symposium
On Turbulence and Shear Flow
Phenomena (TSFP-9)
June 30 - July 3, 2015 *Melbourne, Australia*

A NOVEL VLES MODEL FOR TURBULENT FLOW SIMULATIONS

C.-Y. Chang, S. Jakirlić, B. Krumbein and C. Tropea
Institute of Fluid Mechanics and Aerodynamics / Center of Smart Interfaces
Technische Universität Darmstadt, Alarich-Weiss-Straße 10, D-64287 Darmstadt, Germany
s.jakirlic@sla.tu-darmstadt.de

ABSTRACT

Present computational study focusses on formulation of a VLES (Very Large Eddy Simulation) model. The residual turbulence pertinent to the VLES framework is presently modelled by a near-wall eddy-viscosity model, Hanjalic et al. (2004). In addition to the equations governing the kinetic energy of turbulence and its dissipation rate it solves transport equation for the quantity ζ_{us} ($=\overline{v_{us}^2}/k_{us}$), representing a key parameter as it models the near-wall anisotropy influence on the velocity scale in the expression for the corresponding turbulence viscosity. The VLES method is validated interactively in the process of the model derivation by computing the natural decay of the homogeneous isotropic turbulence (assessed comparatively along with the complementary LES simulations), fully-developed flow in a plane channel and a separating flow over a periodic arrangement of smoothly-contoured 2-D hills in a Reynolds number range. In addition all considered flows are simulated by using the same RANS (Reynolds-averaged Navier-Stokes) model representing the constituent of the VLES method.

INTRODUCTION

A computational strategy employing a RANS-based (RANS – Reynolds-Averaged Navier Stokes) model formulation to describe the sub-scale turbulence in an LES-relevant (LES – Large-Eddy Simulation) procedure experiences increased popularity in last years, see e.g. Jakirlic and Maduta (2015). The goal is to combine the advantages of both RANS and LES methods aiming at providing a computational procedure that is capable to affordably capture the fluctuating turbulence. This is of decisive importance in e.g. configurations featured by flow separated from curved continuous walls (characterized by intermittent separation region). The fluctuating turbulence associated with the separated shear layer has to be appropriately resolved in order to capture even the mean flow properties.

The work reported here aims primarily at validation of a seamless hybrid LES/RANS method denoted as VLES (in line with Speziale, 1998) in several generic attached and separated flow configurations in a range of Reynolds numbers; the VLES method is concerned with appropriate suppression of the turbulent viscosity in the equation of motion directly. The VLES method captures the unsteady turbulent flow features more accurately compared to the conventional URANS (Unsteady RANS) method.

COMPUTATIONAL METHOD

The present modelling activities are concerned with the VLES scheme formulation representing a seamless hybrid LES/RANS model providing a smooth transition from RANS to LES. Accordingly, the turbulence associated with the non-resolved residual motion is represented by the residual stress tensor as follows

$$\widetilde{\tau_{ij}} = F_r\, \tau_{ij}^{RANS} \qquad (1)$$

The function F_r blends between the DNS (Direct Numerical Simulation) mode ($F_r \to 0$; $\Delta \sim \eta_K$, with $\eta_K = (\nu^3/\varepsilon)^{1/4}$ denoting the dissipative Kolmogorov scales) and pure RANS ($F_r \to 1$; $\tau_{ij}^{RANS} \equiv \overline{u_i u_j}$; $\Delta \sim k^{3/2}/\varepsilon$, with $k = \overline{u_i u_i}/2$ and ε representing the kinetic energy of the RANS turbulence and its dissipation rate). Herewith, the fully-modelled RANS mode will be seamlessly bridged to fully-resolved DNS in accordance with the vanishing $\widetilde{\tau_{ij}}$. Between these two limits an LES or a VLES will be recovered. In the LES, the largest modelled ('u' - unresolved) length scale ($\Lambda_u = k_u^{3/2}/\varepsilon_u$) is proportional to the grid spacing: $\Delta \sim \Lambda_u$. Accordingly

$$\Delta = \frac{k_u^{3/2}}{\varepsilon_u} = \frac{F_k^{3/2} k_{us}^{3/2}}{F_\varepsilon \varepsilon_{us}} = \frac{F_k^{3/2}}{F_\varepsilon} \Lambda_{us} \qquad (2)$$

with the ratios (actually resolution parameters) $F_k = k_u/k_{us}$ and $F_\varepsilon = \varepsilon_u/\varepsilon_{us}$ adopted from the PANS methodology (Basara et al., 2011). Analogous to PANS F_ε can be taken as unity ($\varepsilon_u = \varepsilon_{us}$). The present VLES method employs the Unsteady RANS model applying a built-in function F_r to appropriately suppress the relevant turbulent viscosity (ν_{us}) to the sub-grid scale level ν_u, i.e. $\nu_u = F_r \nu_{us}$. If adopting a $k-\varepsilon$-type model to define the turbulent viscosity ($\nu_t \sim k^2/\varepsilon$) the function F_r reduces to

$$F_r = \frac{k_u^2}{k_{us}^2} = F_k^2 = \left(\frac{\Delta}{\Lambda_{us}}\right)^{4/3} \Rightarrow F_r = \min\left[\left(\frac{\Delta}{\Lambda_{us}}\right)^{4/3}, 1\right] \qquad (3)$$

In the flow regions where the modelled length scale is smaller than the filter width ($\Lambda_{us} \le \Delta$), the 'unsteady' ('us') turbulent properties become equivalent to the fully-modelled properties, implying the URANS operating mode of the VLES method prevails: $F_k = F_r = 1$, Fig. 1. The presently employed VLES method utilizes the near-wall $\zeta - f$ model formulation, Hanjalic et al. (2004), as the background URANS model scheme. In addition to the equations governing the kinetic energy of turbulence k_{us} and its dissipation rate ε_{us} it solves transport equations for the quantity ζ_{us} , representing the ratio $\overline{v_{us}^2}/k_{us}$, and elliptic function f, with $\overline{v_{us}^2}$ denoting the scalar variable

which behaves as the normal-to-the-wall Reynolds stress component by approaching the solid wall. Accordingly, ν_u reads

$$\nu_u = F_r \nu_{us} = F_r C_\mu^\zeta \zeta_{us} k_{us} T_{us} \qquad (4)$$

The 'us' turbulent quantities relate to the residual turbulence of the VLES method. T_{us} is a corresponding time scale switch, Eq. (5).

$$T_{us} = \max\left[C_\tau \left(\frac{\nu}{\varepsilon_{us}} \right)^{1/2}, \frac{k_{us}}{\varepsilon_{us}} \right] \qquad (5)$$

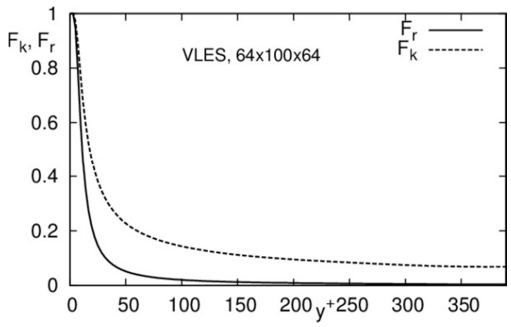

Figure 1. Profiles of the functions F_k and F_r (Eq. 3) in a fully-developed channel flow at $Re_\tau = 395$

Detailed specification of the VLES model is given in Chang et al. (2014). Both RANS-$\zeta - f$ and the present VLES models are implemented into the CFD software package OpenFOAM® with which all present simulations were performed. All flow configurations were computed by using the 2nd order central differencing scheme (CDS) employed in a differed correction manner. Temporal discretization is accomplished by the 2nd order accurate Crank-Nicolson scheme. Despite the fact that the grid resolutions used for all wall-bounded flow configurations considered presently enable applications of exact wall-boundary conditions, the near-wall VLES model is presently applied in conjunction with the universal wall treatment. This method blends the integration up to the wall with the standard equilibrium wall functions, enabling well-defined boundary conditions irrespective of the position of the wall-closest computational node. The approach used here (Basara et al., 2007) represents a somewhat modified "compound wall treatment" proposed by Popovac and Hanjalic (2007). Accordingly, relevant quantities (wall shear stress, production and dissipation of the turbulent kinetic energy) are represented by a blending formula specified at the central node P of the wall-closest grid cell.

RESULTS AND DISCUSSION

The predictive capabilities of the present VLES model are illustrated by computing some generic attached and separating flow configurations including a plane channel flow (reference Direct Numerical Simulation is from Moser et al, 1999) and flow over a periodical arrangement of smoothly-curved 2D hills (reference LES simulations and experiments are by Breuer et al., 2009 and Rapp and Manhart, 2011). The natural decay of homogeneous isotropic turbulence (HIT) in accordance with the DNS of Jimenez (see Tavoularis et al., 1997, AGARD Advisory Report 345; http://torroja.dmt.upm.es/turbdata/agard/) is preliminary computed in course of the model development. A selection of relevant results is displayed in Figs. 2-**14**.

The VLES model validation by means of the HIT benchmark is performed at the Taylor-microscale-based Reynolds number $Re_\lambda = 104$. A cube-shaped solution domain whose volume corresponds to $(2\pi)^3$ is meshed by the three grids comprising 128^3; 64^3 and 32^3 cells. The initial sub-grid scale properties are estimated by interpolating the LES data provided also by Jimenez at a grid consisting 128^3 cells. For two lower grid resolutions the initial fields of the residual turbulence (as well as the temporal developments of the associated kinetic energy, e.g. Fig. 3-lower) are obtained by integrating the DNS (performed at a grid consisting of 512^3 cells) energy spectrum, e.g. Fig. 3-upper. The unresolved (sub-grid scale) turbulent kinetic energy and corresponding dissipation rate can be estimated from the turbulent viscosity formulation (Pope, 2000, pp. 630-631) reading:

$$k_u = \left(C_S^2 \Delta / C_D \right)^2 \left| \overline{S} \right|^2, \quad \varepsilon_u = C_E k_u^{3/2} / \Delta \qquad (6)$$

with $C_S = 0.1$, $C_D = 0.094$ and $C_E = 0.9 - 1.1$. The VLES predictive performances with respect to the model behavior under the influence of grid coarsening/refinement are analyzed along with the outcome of an LES simulation (performed presently for the purpose of comparison with the VLES-results). Fig. 2 illustrates the vortex structure obtained by both LES and VLES at the final time sequence corresponding to t=1.5 s.

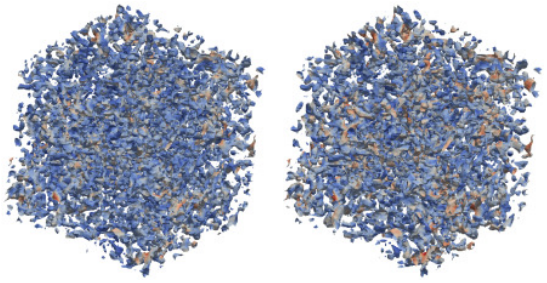

LES VLES

Figure 2. HIT decay: Q invariant (Q = 2.5 s^{-2}) of instantaneous velocity field at the final time sequence t=1.5 s; mesh resolution: 64^3

The energy spectrum corresponding to the time sequence t=1.45 s obtained by the present VLES method for the coarsest and finest grid sizes is depicted in Figs. 3-4-upper illustrating good agreement with the reference DNS. In addition the temporal evolution of the unresolved (sub-grid scale) turbulent kinetic energy compared to the corresponding DNS data (corresponding to relevant spectral cut-offs) is also shown. The LES simulations utilizing the conventional Smagorinsky model underestimate substantially the sub-grid scale turbulent properties at two coarser meshes consisting of 64^3 (not shown here) and 32^3 cells; we recall here that the

Smagorinsky SGS model works well only if a grid resolution is of appropriate size implying the spectral cut-off being positioned well in the inertial sub-region characterized by the slope $\kappa^{-5/3}$. Unlike the present VLES results, following closely the DNS data for all three grid sizes (Figs. 3-4), the LES returned reasonably the DNS results only at the finest grid resolution corresponding to 128^3 grid cells.

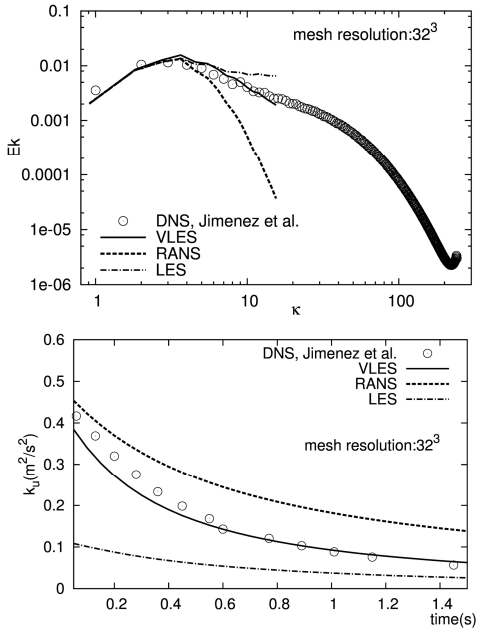

Figure 3. HIT decay: turbulence energy spectrum at t=1.45 s (upper) and temporal evolution of unresolved turbulent kinetic energy (lower); mesh resolution: 32^3

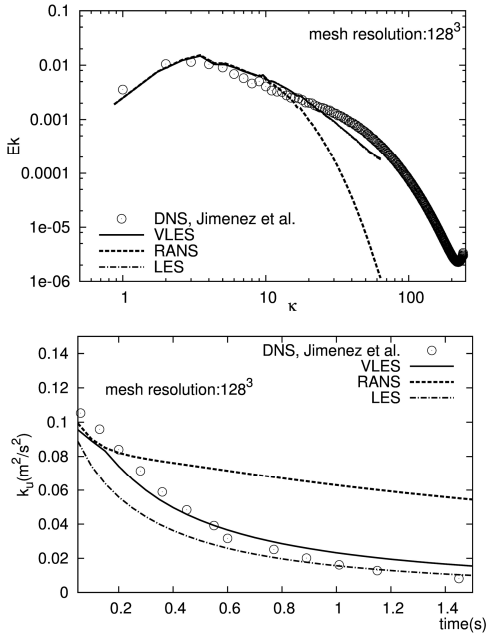

Figure 4. HIT decay: turbulence energy spectrum at t=1.45 s (upper) and temporal evolution of unresolved turbulent kinetic energy (lower); mesh resolution: 128^3

The next case considered, a fully-developed flow in a plane channel underlying the logarithmic law for the velocity field, represents the most important flow configuration for studying the near-wall turbulence. The solution domain adopted for the presently studied channel flows at $Re_\tau = 395$ ($L_x \times L_y \times L_z = 4h \times 2h \times 2h$; with h representing the half channel width) was meshed by three grids comprising (N_x, N_y, N_z)=(64, 100, 64), (48, 80, 48) and (40, 70, 40) grid cells. The finest grid implies the resolution corresponding to $\Delta x^+ = 25$ and $\Delta z^+ = 12.5$; the height of the wall-next grid cell is $\Delta y^+ = 1.8$. The VLES simulation started from the mean flow and turbulence fields obtained by the $\zeta - f$ model within the steady RANS framework. The final outcome corresponds to an appropriate instantaneous flow field visualized by the Q-criterion in Fig. 5.

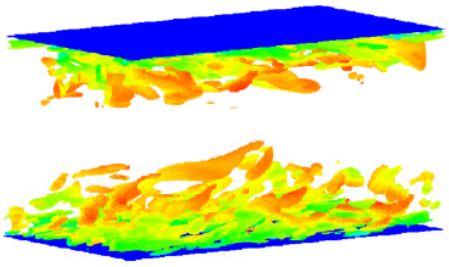

Figure 5. Channel flow at $Re_\tau = 395$: vortex structure visualized by Q-criterion (Q=0.005 s^{-2})

Fig. 6 displays the profiles of the total and unresolved (subgrid) fraction of the kinetic energy of turbulence for all three grid resolutions tested. Reduction of the unresolved turbulence intensity (Eq. 6), with the maximum concentrated to the near-wall region, in terms of grid coarsening is obvious. The profiles of the mean velocity and all four Reynolds stress components exhibit very good agreement with the DNS results of Moser et al. (1999), Fig. 7. Reasonable results are obtained also for coarser grid resolutions, Fig. 6 and 7-upper. Herewith, good predictive capabilities of the present VLES model in capturing the fluctuating turbulence also in such a globally stable flow with no inherent forcing are illustrated. It is furthermore demonstrated that even an eddy-viscosity model, if appropriately adjusted as the constituent of a hybrid LES/RANS modelling strategy, can correctly return all Reynolds stress components.

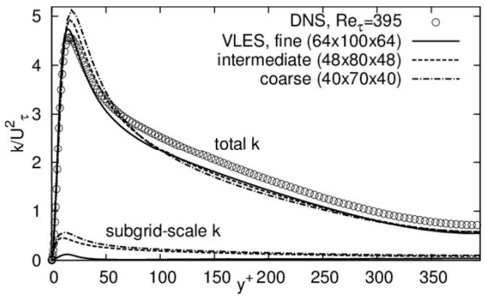

Figure 6. Channel flow at $Re_\tau = 395$: profiles of the kinetic energy of turbulence

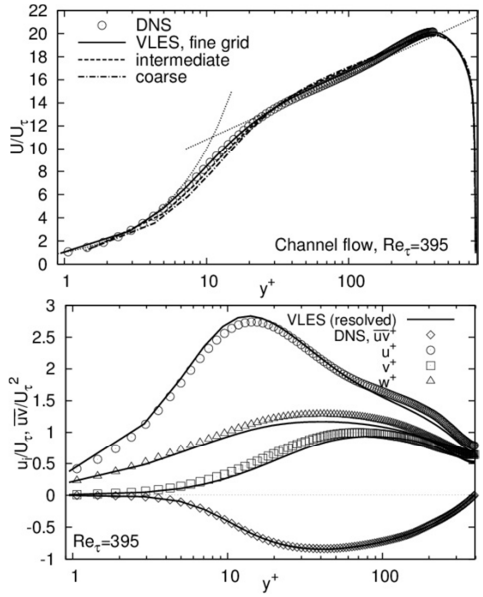

Figure 7. Channel flow at $Re_\tau = 395$: mean velocity and Reynolds stress component profiles (the latter results relate to the finest grid applied)

In addition, the fully-developed channel flow at significantly higher Reynolds number $Re_\tau = 2003$ is also computed by the present VLES. The solution domain, corresponding to that used for the low Reynolds number case, is meshed by $(N_x, N_y, N_z) = (128, 100, 128)$ grid cells. The wall-next grid cell is positioned at the edge of the viscous sublayer at $y^+ \approx 5$. Figs. 8 display the profiles of the total and unresolved (subgrid) kinetic energy of turbulence as well as the mean velocity profile.

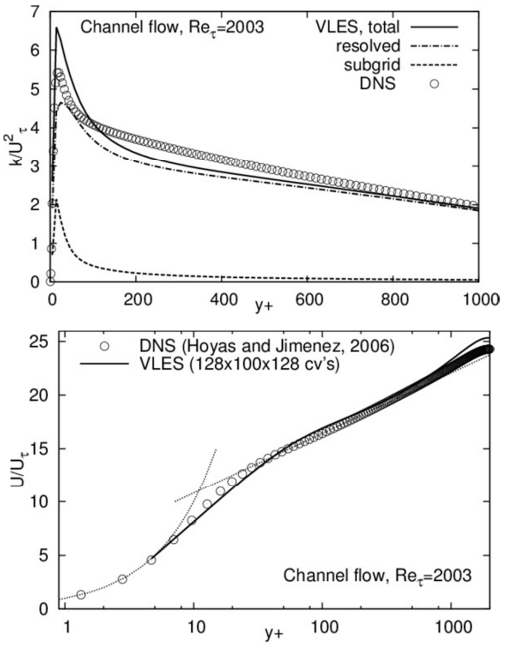

Figure 8. Channel flow at $Re_\tau = 2003$: profiles of the kinetic energy of turbulence and mean velocity

The flow over a 2D hill ($L_x \times L_y \times L_z = 9H \times 3.03H \times 4.5H$; with H representing the hill height; Fig. 9) at $Re_H = 10600$ and $Re_H = 37000$ was computed by using the mesh comprising (N_x, N_y, N_z)=(80, 100, 30) and (N_x, N_y, N_z)=(160, 160, 60) grid cells, making in total 240000 and 1.5 million grid cells respectively. Flow at both Reynolds numbers has been experimentally investigated by Rapp and Manhart (2011). In addition, a reference LES by Breuer et al. (2009) is made available for the flow at $Re_H = 10600$. It is interesting to report that no initial field fluctuations in these periodical flows were necessary. The fields obtained by the steady RANS computations using the $\zeta - f$ model served for the initialization of the computations with the present VLES-$\zeta - f$ formulation. Both simulations resulted in an instantaneous flow field, see Fig. 10. The F_k-field (Eq. 3) depicted in Fig. 11 exhibits the values well under 1 in the entire flow domain (it is recalled that $F_k = 1$ implies the RANS operating mode), illustrating high portion of the resolved flow despite very coarse grid resolution.

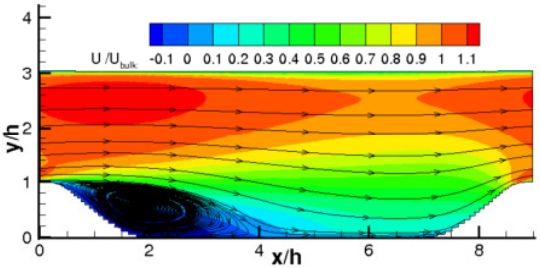

Figure 9. Time-averaged velocity field and corresponding streamline pattern obtained by VLES at $Re_H = 10600$

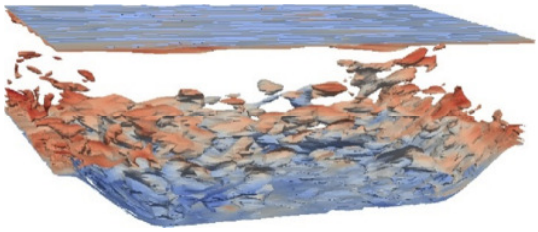

Figure 10. 2D hill flow: flow structure visualized by vorticity at $Re_H = 10600$

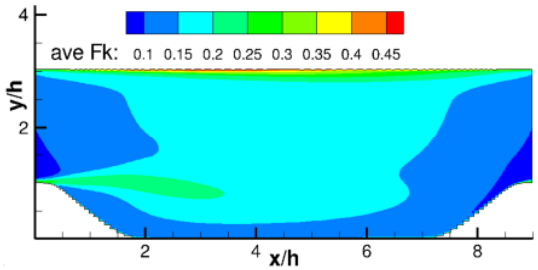

Figure 11. 2D hill flow at $Re_H = 10600$: iso-contours of the resolution parameter $F_k = k_u/k_{us}$ (Eq. 3)

The 2D hill configuration exhibits numerous features associated with the flow separation at a curved continuous

surface characterized by a high level of natural instability, originating primarily from the highly intermittent separation region which oscillates over a wider wall area. Consequently a typical outcome of any RANS model (we recall that the application of a conventional RANS model applied in the Unsteady RANS framework results in a steady solution), almost independent of the modeling level, is a low intensity of the turbulence activity in the separated shear layer resulting in a much larger recirculation zone, Figs. 13-14. Figs. 13-14 display the comparison of the axial velocity and Reynolds shear stress component profiles for both Reynolds numbers considered revealing some Reynolds number dependent features of the velocity and turbulence field. Figs. 13-14-upper reveals the intensified turbulence activity in the separated shear layer (coinciding with the distance to the wall at $y/h \approx 1$) with the Reynolds number increase returned correctly by the present VLES (the shear stress component development, normalized by the velocity value above the hill crest, points out similar turbulence level for both configurations, but an almost four times higher bulk velocity should be recalled with respect to the absolute value of $\overline{uv}$-stress). It is in accordance with an appropriate recirculation zone shortening illustrated clearly by the friction factor development (Fig. 12) and velocity profile evolution agreeing well with reference database, Figs. 13-14-lower.

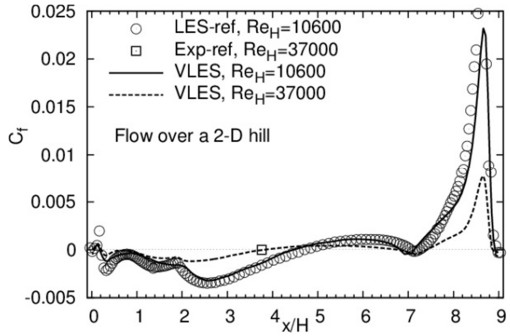

Figure 12. 2D hill flow: friction factor development at the lower wall for both Reynolds numbers

CONCLUSIONS

A VLES model scheme relying on a RANS-based near-wall, four-equation, eddy-viscosity model describing the respective residual turbulence is formulated and validated by computing natural decay of homogeneous isotropic turbulence, attached flow in a plane-channel and the flow separating from a series of smoothly-contoured hills in a Reynolds number range. Whereas the destruction term in the equation governing the scale-supplying variable is appropriately modelled in the most of existing hybrid methods (as e.g. in a PANS framework, Basara et al., 2011), the VLES method is concerned with appropriate suppression of the turbulent viscosity in the equation of motion directly causing appropriate turbulence level suppression towards the 'sub-scale' level. Herewith, the development of the structural characteristics of the flow and associated turbulence is enabled. Accordingly, capturing of important mean flow and turbulence features, being beyond the reach of background RANS model, can also be achieved by using coarser grid resolutions.

REFERENCES

Basara, B., Aldudak, F., Schrefl, M., Jakirlic, S., Hanjalic, K. Tropea, C. and Mayer, J., 2007, "Experimental Investigations and Computations of Unsteady Flow past a Real Car Using a Robust Elliptic Relaxation Closure with a Universal Wall Treatment", *SAE Technical Paper Series*, Paper No. 2007-01-0104 (also in *SAE 2007 Transactions, Journal of Passenger Cars – Mechanical Systems*, March 2008; Vol. V116-6, ISBN: 978-0-7680-1985-8).

Basara, B., Krajnovic, S., Girimaji, S. and Pavlovic, Z., 2011, "Near-Wall Formulation of the Partially Averaged Navier-Stokes (PANS) Turbulence Model", *AIAA Journal*, Vol. 49(12), pp. 2627-2636.

Breuer, M., Peller, N., Rapp, Ch. and Manhart, M., 2009, "Flow over periodic hills - Numerical and experimental study in a wide range of Reynolds numbers", *Computers and Fluids*, Vol. 38, pp. 433-457.

Chang, C.-Y., Jakirlic, S., Dietrich, K., Basara, B. and Tropea, C., 2014, "Swirling flow in a tube with variably-shaped outlet orifices: an LES and VLES study", *Int. J. Heat and Fluid Flow*, Vol. 49, pp. 28-42.

Hanjalic, K., Popovac, M. and Hadziabdic, M., 2004, "A robust near-wall elliptic-relaxation eddy-viscosity turbulence model for CFD", *Int. J. Heat and Fluid Flow*, Vol. 25(6), pp. 1047-1051.

Hoyas, S. and Jimenez, J., 2006, "Scaling of the velocity fluctuations in turbulent channels up to $Re_\tau = 2003$", Phys. Fluids, Vol. **18** (011702)

Jakirlić, S. and Maduta, R., 2015, "Extending the bounds of "steady" RANS closures: towards an instability-sensitive Reynolds stress model", *Int. J. Heat and Fluid Flow*, Vol. 51, pp. 175-194.

Moser, R.D., Kim, J. and Mansour, N.N., 1999, "Direct numerical simulation of turbulent channel flow up to $Re_\tau = 590$", *Physics of Fluids*, Vol. 11(4), pp. 943-945.

Rapp, C. and Manhart, M., 2011, "Flow over periodic hills: an experimental study", *Experiments in Fluids*, Vol. 51, pp. 247-269.

Popovac, M. and Hanjalic, K., 2007, "Compound wall treatment for RANS computation of complex turbulent flows and heat transfer", *Flow Turbulence and Combustion*, Vol. 78, pp. 177–202.

Speziale, C.G., 1998, "Turbulence modeling for time-dependent RANS and VLES: a review", AIAA J., Vol. 36 (2), pp. 173–184.

Tavoularis, S., Jimenez, J., Leuchter, O., 1997, "A Selection of Test Cases for the Validation of Large-Eddy Simulations of Turbulent Flows – Homogeneous Flows", AGARD Advisory Report No 345, Working Group 21 of the Fluid Dynamics Panel of AGARD (http://torroja.dmt.upm.es/turbdata/agard/)

Acknowledgement. The financial support of the German Scientific Council (Deutsche Forschungs-gemeinschaft - DFG) in the framework of the SFB-TRR 150 (TP-B03) project is gratefully acknowledged.

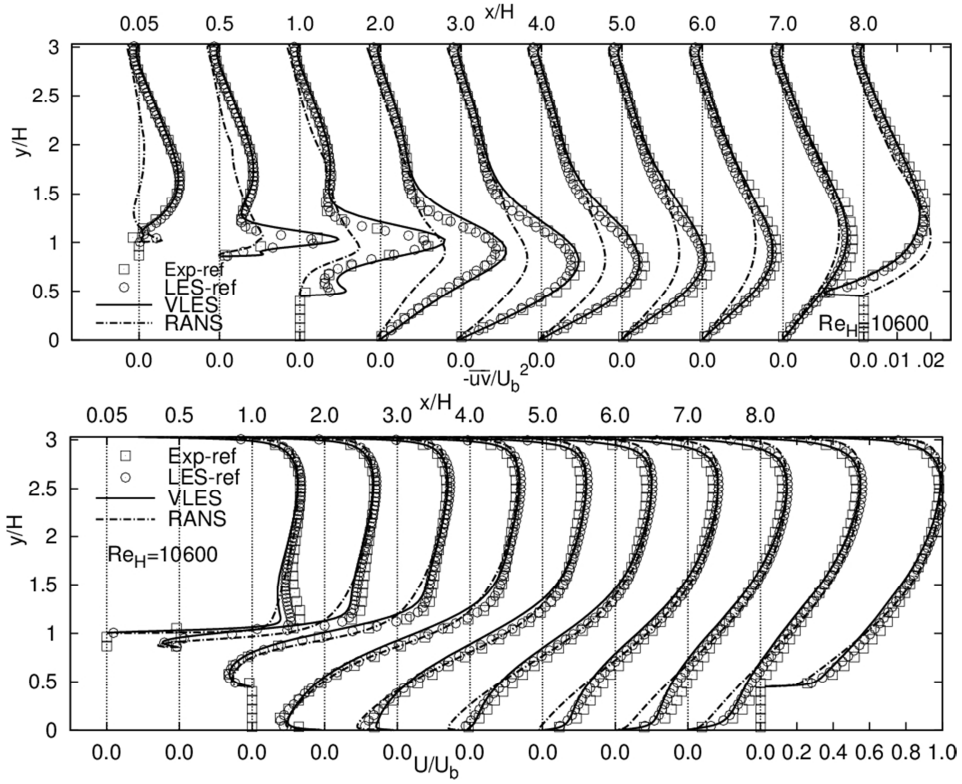

Figure 13. 2D hill flow: Reynolds shear stress and axial velocity profile developments at $Re_H = 10600$

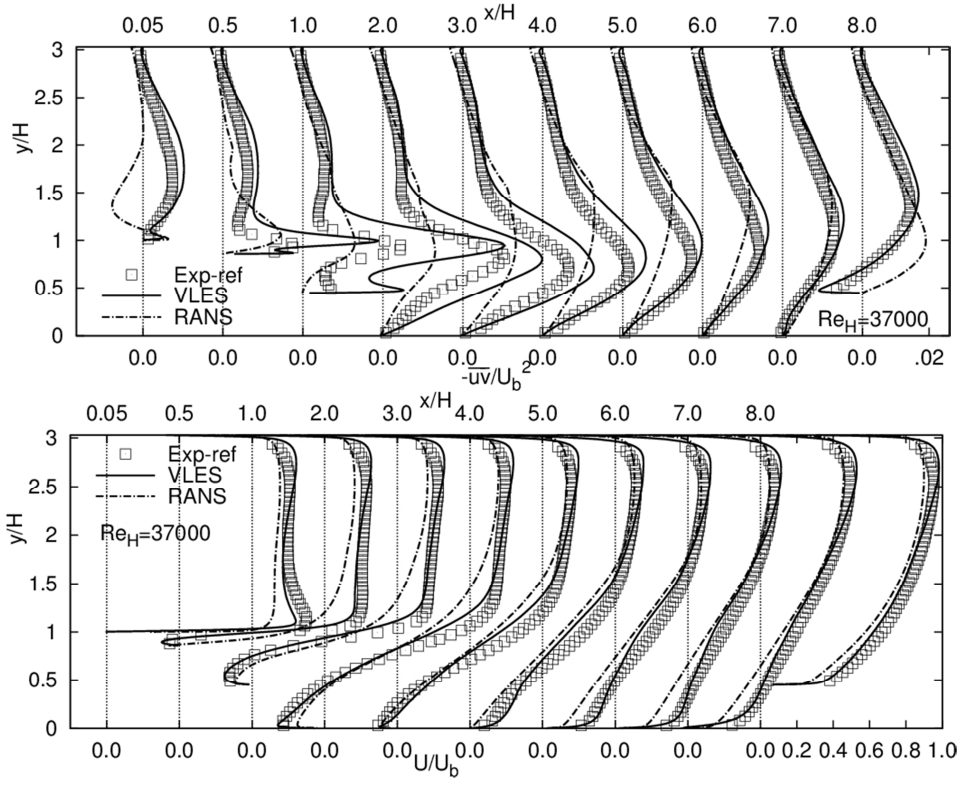

Figure 14. 2D hill flow: Reynolds shear stress and axial velocity profile developments at $Re_H = 37000$